QUALIFICATION PROCEDURE OF LUMINAIRES IN THE EVENT OF AN IMPACT TO THE POLE

Frédéric MARIN*, Christian MARVILLE**, Jean-Claude GOLINVAL***

*V2i s.a.
Boulevard de Colonster, 4 B56 (PIMW) B-4000 Liège
**R-TECH, Schréder Group GIE
Rue de Mons, 3 B-4000 Liège
*** University of Liège, Department of Aerospace and Mechanical Engineering,
LTAS – Vibrations et Identification des Structures
Chemin des chevreuils, 1 B52/3 B-4000 Liège
e-mails: f.marin@v2i.be, christian.marville@rtech.be, jc.golinval@ulg.ac.be

Abstract: The objective of the study is to develop a testing specification on an electrodynamic shaker which ensures the qualification of a parking lighting device, whose pole is impacted by a car. The methodology is based on both a numerical approach and an experimental approach using an electrodynamic shaker. The first step of the analysis consists in modeling the structure and the excitation by means of a finite element approach. The calculation of the dynamic response of the "pole/lighting device" system to impact loading is repeated for different geometries of the pole. The second step is to consider each dynamic response at the fixing point of the lighting device on the pole as input for a base-excited single degree of freedom system. The theory developed for such a system allows to define severity criteria like the Shock Response Spectrum (SRS) which is the most representative criterion in the case of an impact. The severity of the vibration environment of the lighting device is then obtained by considering the envelope of the different computed SRS. Finally, different test specifications leading to equivalent SRS are proposed and the device is tested on an electrodynamic shaker. The developed methodology was applied to the NEMO lighting device (Schréder).
Keywords: Lighting device, impact, pole, electrodynamic shaker, finite element, SRS, ERS, specification

1. Model of the "pole/luminaire" System

The first step of the numerical approach consists in modeling the structure and the excitation by means of the finite element method. For this purpose, the pole is discretized using beam elements and the lighting device is modeled as a rigid body with a concentrated mass as illustrated in Fig. 1.
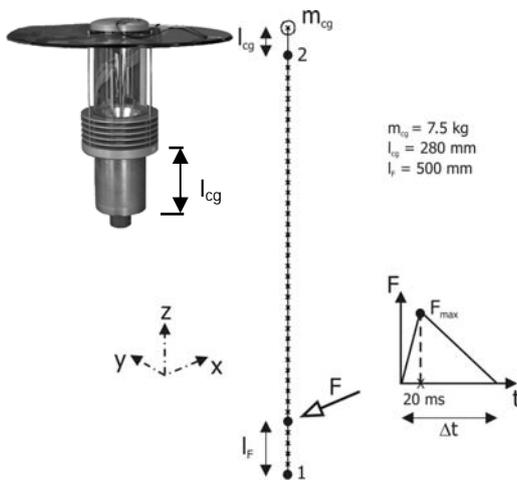
Fig. 1. Finite element model of the *NEMO* "pole/lighting device" system subject to an impact

The general dynamic equilibrium equations of the system take the form :

$$\mathbf{M}\,\ddot{\mathbf{x}}(t) + \mathbf{C}\,\dot{\mathbf{x}}(t) + \mathbf{K}\,\mathbf{x}(t) = \mathbf{f}(t) \qquad (1)$$

where $\mathbf{M}$, $\mathbf{C}$, $\mathbf{K}$ are respectively the mass, damping and stiffness matrices;

$\mathbf{x}$, $\dot{\mathbf{x}}$ and $\ddot{\mathbf{x}}$ are the displacement, speed and acceleration vectors;

$\mathbf{f}$ is the vector of external forces applied to the structure.

The excitation is determined both from experimental observations performed in a real case on the *NEMO* lighting device manufactured by *Schréder* (Fig. 1), and from information collected in references [2] and [7]. It appears, on one hand, that the structural integrity of the pole is not affected by the impact and, on the other hand, that the car-pole collision can be represented by an impact force F(t) whose time evolution has the shape of a triangle of height F_{max} and base Δt (Fig. 1). According to references [2] and [7], the maximum of the excitation force generally occurs after 20 ms and the duration of the impact varies from 80 to 200 ms depending on the deformation caused to the car. Knowing the mass m of the car as well as its initial speed v_{ini} (Tab. 1), the *principle of linear impulse and momentum* gives :

$$\int_0^{\Delta t} F(t)\, dt = m \left| v_{end} - v_{ini} \right| \qquad (2)$$

i.e. for a zero speed after impact ($v_{end} = 0$) :

$$F_{max} = \frac{2\, m\, v_{ini}}{\Delta t} \qquad (3)$$

Simulation	m [kg]	Δt [ms]	v_{ini} [m/s]	F_{max} [kN]
1	900	200	5.6	50.0
2	900	200	9.7	87.2
3	900	80	5.6	125.0
4	900	80	9.7	218.2

Tab. 1. Computation of the maximal impact force for given m, Δt and v_{ini}

2. Dynamic Response of the "pole/luminaire" System

The computation of the dynamic response of the structure to an impact is performed using the finite element software *Samcef* [9] and consists of a transient computation based on the *mode acceleration method* [3].

The geometric data of the different steel poles on which the *NEMO* lighting device may be mounted are summarized in Tab. 2. In view of its frequent use and its weak clamping section, pole n°1 is considered here as the reference pole. It is used here to correlate the computation results with the observations collected on the real test-case.

Pole	Height [m]	$\varnothing_{top}$ [mm]	$\varnothing_{base}$ [mm]	Thickness [mm]	Rate of use
1	4	60	116	3	frequent
2	4	76	132	3	less frequent
3	5	60	130	3	frequent
4	5	62	132	4	less frequent
5	5	62	147	4	rare
6	5	76	147	3	rare
7	4	76	144	3	frequent
8	5	76	144	3	frequent
9	4	60	110	3	rare
10	5	60	123	3	rare

Tab. 2. Geometric data of the *NEMO* steel poles

Based on the assumption that the pole is not damaged by the impact, the maximum allowable force F_{max} is calculated to be equal to 15 kN, which corresponds to an initial speed of 2.5 to 6 km/h, depending on the impact duration. Depending on the considered damping ratio (from 0.05% to 5%), the acceleration level at the fixing point of the lighting device (point 2 in Fig. 1) varies from 90 to 164 m/s².

For example, the time signals of the stress computed at point 1 and of the corresponding acceleration at point 2 for a damping ratio of 0.05 % (conservative value which is equivalent to the application of a security factor) are given in Fig. 2.
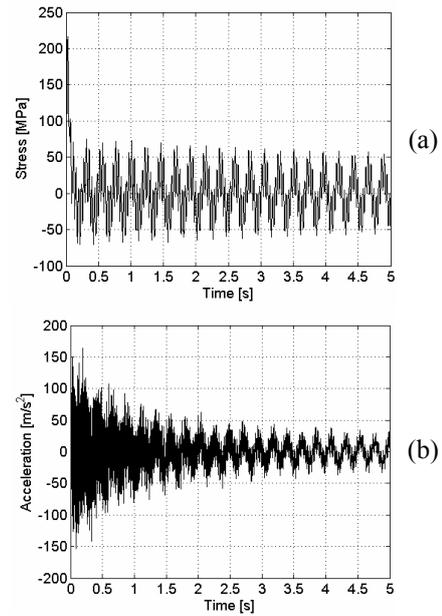
Fig. 2. Dynamic response of pole n°1 ($\varepsilon = 0.05$ %) : (a) Stress at point 1; (b) Acceleration at point 2 in the *ox* direction

The computation is then repeated for each pole considered in Tab. 2. The peak responses in terms of stress at the base of the pole (point 1) and of the acceleration at the connection of the lighting device on the pole (point 2) are shown in Fig 3.
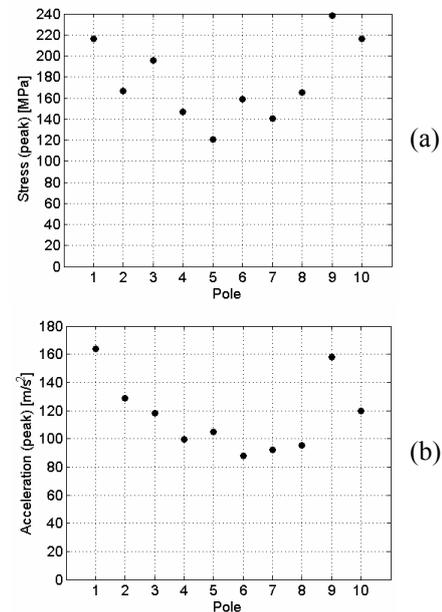
Fig. 3. Peak responses computed for the whole set of *NEMO* poles ($\varepsilon = 0.05$ %) : (a) Stress at the base of the pole (point 1); (b) Acceleration at the fixing point of the lighting device on the pole (point 2) in the *ox* direction

It can be noticed that the highest stress (238 MPa) slightly exceeds the yield strength of steel but appears at the base of the weakest pole (pole n°9) which is however

rarely used. The most important acceleration (17 g) is observed at the fixing point of the lighting device on pole n°1.

3. Severity of the Luminaire Vibration Environment

Once the acceleration at the fixing point of the lighting device (point 2) caused by the impact excitation has been determined for each pole, it can be used as the excitation applied at the base of a reference single degree of freedom system (Fig. 4) with the aim of calculating the *Shock Response Spectrum* (*SRS*) [1]. The damping ratio of the active eigenmode of the lighting device being unknown, a usual value of 5 % has been considered [5]. The frequency bandwidth considered for the analysis ranges from 0 to 55 Hz and contains the main natural frequencies of the lighting device.
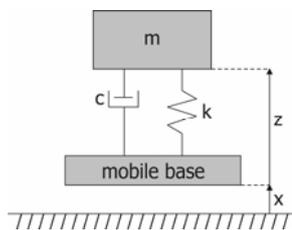
Fig. 4. Base-excited single degree of freedom system

The specification representing the vibration environment of the lighting device further to an impact on the pole is then obtained taking the envelope of all the computed *SRS*, Fig. 5 (a). A simplified but conservative envelope is also determined to be used as input for the control system of an electrodynamic shaker, Fig. 5 (b).
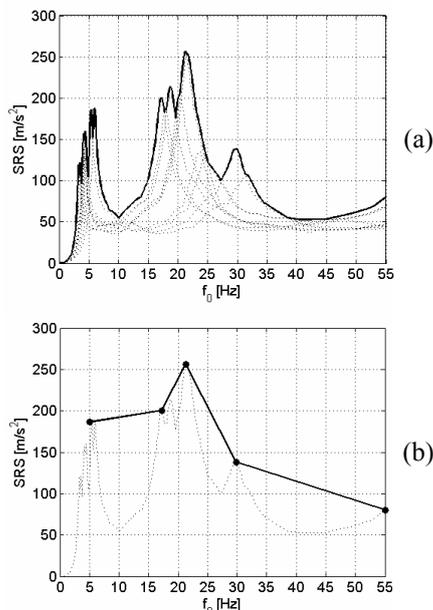
Fig. 5. Testing specification equivalent to an impact on the pole : (a) Envelope of the *SRS* computed from the responses of the different poles at the fixing point of the lighting device for ε = 5 %; (b) Envelope to be used for vibration testing on electrodynamic shaker

SRS Specification

Electrodynamic shakers are always piloted by a time sample. There actually exists an infinity of time samples satisfying the *SRS* defined in Fig. 5. An example of a possible control signal synthesized from the envelope shown in Fig. 5 (b) is given in Fig. 6.
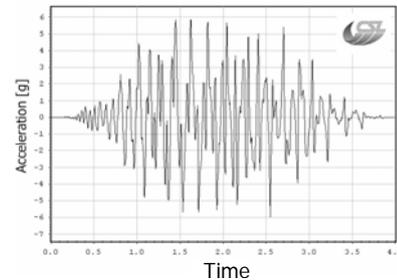
Fig. 6. Example of time sample corresponding to the *SRS* of Fig. 6 (b) (generated with the *VibExec* vibration control system, *m+p international*, provided by *CSL – University of Liège*)

If such a *Shock Response Synthesis* module [8] is not available, alternative specifications based on common excitation profiles (e.g. shock, sine sweep and random signal) may be defined.

Shock Specification

Two examples of shock specifications are illustrated in Fig. 7 and their corresponding *SRS,* computed by means of the single degree of freedom approach [5], are compared in Fig. 8. The parameters describing the theoretical pulses to envelop the reference spectrum are listed in Tab. 4.
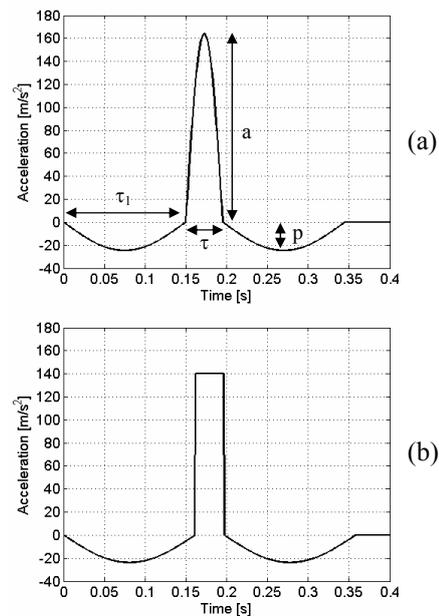
Fig. 7. Examples of shock specification (a = peak pulse, τ = pulse length, p = pre/post pulse amplitude, τ_1 = pre/post pulse length) : (a) Half-sine/single sided pulse; (b) Rectangular pulse
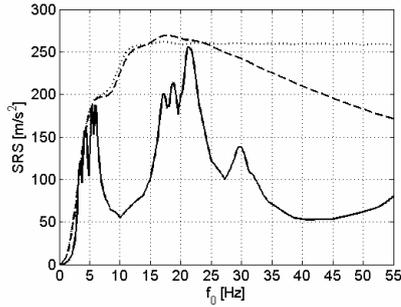
Fig. 8. Comparison between the *SRS* of shock specifications and of the vibration environment of the *NEMO* lighting device for ε = 5 % (- - -, Half-sine/single sided pulse; · · ·, Rectangular pulse; —, Envelope of the computed *SRS*)

	Pulse type	
	Half-sine	Rectangular
a [m/s^2]	164	140
τ [ms]	45	35
p [/]	0.15	0.17
τ$_1$ [ms]	τ/(2p)	(πτ)/(4p)

Tab. 4. Parameters of the shock specifications

Sine Sweep Specification

In the case of a sine sweep excitation, Fig. 9 (a), the theory of the single degree of freedom system allows the computation of the *Extreme Response Spectrum* (*ERS*) [1], [4]. The severity of the sine sweep environment is compared to the *SRS* of the reference spectrum in Fig. 9 (b) and the parameters of the sine sweep excitation are listed in Tab. 5 (note that the indicated sweep rate has been chosen arbitrarily).
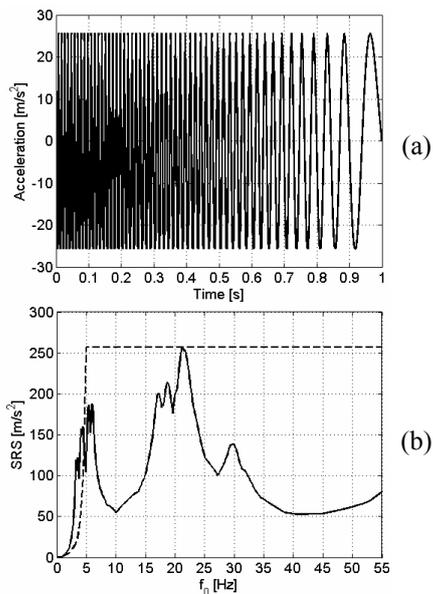
Fig. 9. Example of sine sweep excitation: (a) Control time sample; (b) *ERS* and *SRS* for ε = 5 % (- - -, Sine sweep excitation; —, Envelope of the computed *SRS*)

	Sine sweep (down)
Amplitude (0-peak) [m/s^2]	25.6
Frequency bandwidth [Hz]	55→5
Sweep rate [Hz/s]	50
Duration [s]	1

Tab. 5. Parameters of the sine sweep specification

Random Specification

The last case considered here consists of a random excitation whose *ERS* is also given by the single degree of freedom system theory [1], [6]. The control time sample and response spectra are shown in Fig. 10 and the specification parameters are listed in Tab. 6 (note that the duration of the test has been chosen arbitrarily).
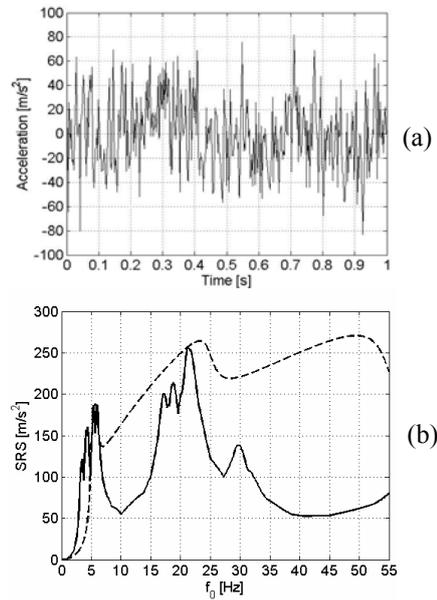
Fig. 10. Example of random excitation: (a) Control time sample; (b) *ERS* and *SRS* for ε = 5 % (- - -, Random excitation; —, Envelope of the computed *SRS*)

	Random		
Amplitude [(m/s^2)^2/Hz]	100	25	10
Frequency [Hz]	[5-6]	[6-25]	[25-55]
Amplitude RMS [m/s^2]	29.8		
Duration [s]	1		

Tab. 6. Parameters of the random specification

4. Experimental Testing on Electrodynamic Shaker

In order to validate the proposed specifications, the *NEMO* lighting device was tested on an electrodynamic shaker. A monoaxial accelerometer ensures the application of the specification in closed loop at the fixing point of the lighting device while a triaxial accelerometer measures the responses of its main body, Fig. 11. When necessary, modifications of the proposed theoretical specifications are presented.

Fig. 11. View of the *NEMO* lighting device ready to be tested on the *Gearing & Watson* 26 kN electrodynamic shaker

Characterization of the Lighting Device

Before each qualification test, a low level sine sweep is generally performed to quickly identify the natural frequencies of the considered specimen. The repetition of such a sweep at the end of the test allows to compare the initial and final states of the structure and therefore to detect a modification of its structural integrity (an important shift in frequency is generally correlated with the apparition of cracks and damage). The parameters defining the sine sweep are given in Tab. 7.

Search for frequencies	
Excitation	Sine sweep
Frequency bandwidth	[5, 55] Hz
Sweep rate	1 oct/min
Acceleration	0.1 g peak

Tab. 7. Specification of the initial and final low level sine sweeps

In the present analysis, the frequency bandwidth has been extended to 200 Hz with the aim of checking that, in the case of a lighting device, the maximal stress is linked to the first mode shape whose frequency is in practice lower than 55 Hz. A strain gage sensitive to the deformations in the *oxz* plane has been therefore stuck on the fixing part as illustrated in Fig. 12. Results in terms of FRFs and stress are also shown in Fig. 12. The interpretation of the results is clear : despite the fact that the amplification factor associated to the first bending mode shape of the lighting device (8.5 Hz) is not the highest one, it nevertheless generates the maximal stress measured in the frequency range [5, 200] Hz (33.5 MPa). Consequently, if a failure happens during the test at qualification level, it will be induced by the first natural frequency of the lighting device. Extrapolating the stress obtained for an excitation of 0.1 g at the fixing point to the test level and comparing with the ultimate stress of the AS12U aluminum (150-200 MPa), it appears that the probability of failure is very important.
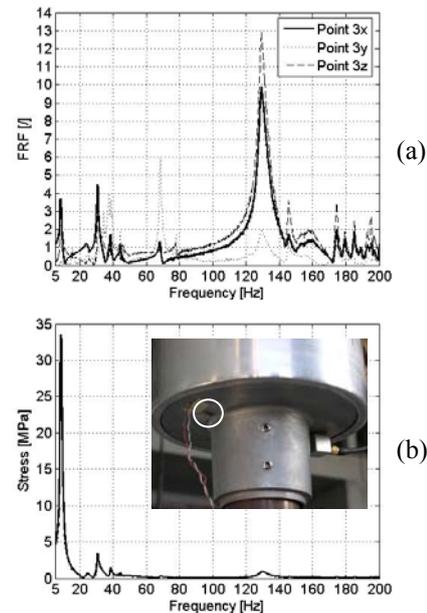
Fig. 12. Low level sine sweep : (a) *FRF* between the responses of the main body (point 3) and the excitation at the fixing point; (b) Stress measured on the external face of the fixing part

Shock Specification

One of the principal drawbacks of the proposed shock specification is the duration of the pulse (35 ms) which requires a prohibitive table displacement (216 mm) for an electrodynamic shaker. On the other hand, a commonly used value of 10 ms associated with an amplitude of 140 m/s^2 leads to an acceptable table displacement of 17 mm. Unfortunately, the resulting *SRS* (Fig. 13) indicates a general decrease of the test severity. Despite the number of pulses at intermediate levels required by the control system, the piloting signal can still be imperfect. Even if its variability decreases with the number of performed intermediate steps, an unexpected damage can occur before the full level is reached. As a result, the severity and reproducibility of the proposed shock specification cannot be guaranteed from one test to another.

Sine Sweep Specification

In the case of the sine sweep specification, the remaining unknown is the sweep rate. As proposed in the theoretical approach, a sweep rate of 50 Hz/s is not conceivable practically because it produces instability in the control loop. Therefore, a compromise between stability of the control system and duration of the test has to be reached. After several attempts, a sweep rate of 1 Hz/s is finally retained. In order not to exceed the authorized displacement of the slip table at low frequency, the control amplitude has been reduced from 25.6 m/s^2 to 18.6 m/s^2 between 5 and 7 Hz. The modified *SRS* is presented in Fig. 14. In spite of the fact that the control spectrum deviates from the reference one

in the frequency range [5, 15] Hz, it appears that the proposed sine sweep specification is able to guarantee a conservative *ERS* in the frequency range [7, 55] Hz.
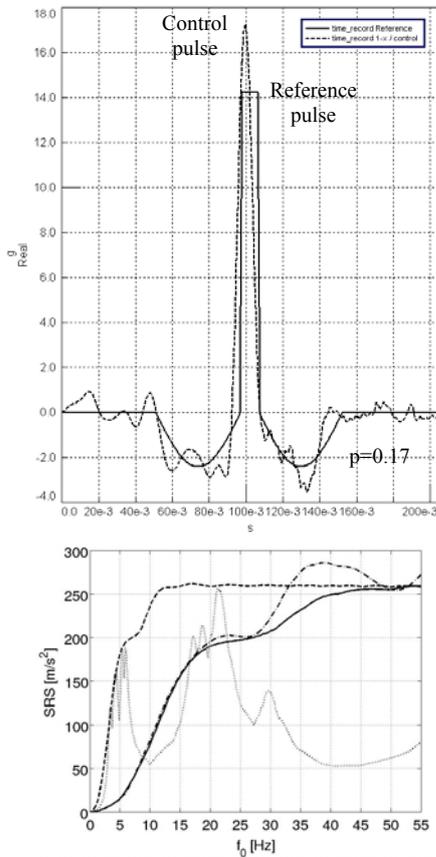
Fig. 13. Rectangular pulses and *SRS* for ε = 5 % :
- - -, Initial specification (a = 140 m/s², τ = 35 ms);
—, Modified specification (a = 140 m/s², τ = 10 ms);
· - ·, Control specification; · · ·, Envelope of the computed *SRS*

Random Specification

The practical difficulties encountered with the random specification are twofold:

- ❑ As discussed in the case of a shock specification, time has to be spent at intermediate levels in order to guarantee a control spectrum which fits correctly the reference spectrum at full level;
- ❑ The excitation duration imposed at full level influences the damage induced to the structure and consequently the severity of the test.

Even if the number and the duration of the intermediate levels are reduced, it may happen that the structure becomes already damaged before the test itself. In order to keep the displacement of the slip table at low frequency within the shaker capabilities, the definition of the control *Power Spectral Density* is started at 7 Hz instead of 5 Hz. An example of control *PSD* is presented in Fig. 15 and its corresponding *ERS* is compared to the theoretical one. Note however that the problem due to

the choice of a suitable duration for the excitation makes difficult the interpretation of the test results.
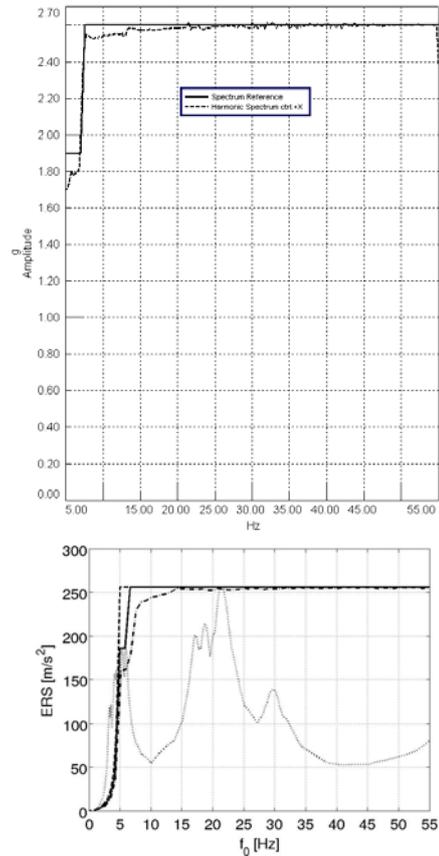
Fig. 14. Sine sweep specifications and *ERS* for ε = 5 %
(- - -, Initial specification; —, Modified specification;
· - ·, Control specification; · · ·, Envelope of the computed *SRS)*

5. Conclusion

According to the previous considerations on the possible test specifications, the sine sweep specification described in Tab. 8 was retained because of its reproducibility as well as its representativeness. As predicted by the simulated results, the failure of the fixing piece was observed experimentally in the real case of the *NEMO* lighting device as shown in Fig. 16.

	Sine sweep (down)
Amplitude (0-peak) [m/s²]	25.6 18.6
Frequency bandwidth [Hz]	55→7→5
Sweep rate [Hz/s]	1
Duration [s]	50

Tab. 8. Parameters of the final sine sweep specification
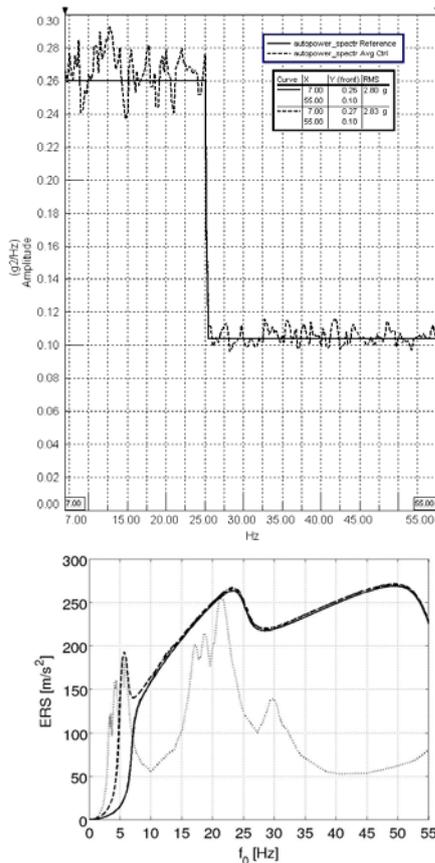
Fig. 15. Random specifications and *ERS* for ε = 5 %
(- - -, Initial specification; —, Modified specification;
· - ·, Control specification; · · ·, Envelope of the
computed *SRS)*
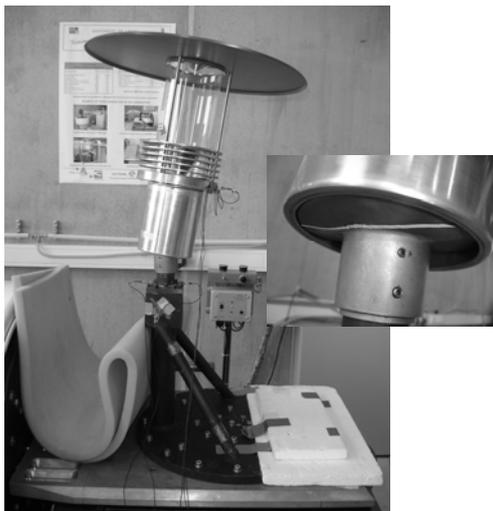
Fig. 16. View of the failure induced to the *NEMO*
lighting device at the end of the "impact test"

6. References

[1] F. CAMBIER, P. DEHOMBREUX, O. VERLINDEN and C. CONTI 1997 *European Journal of Mechanical Engineering* **Vol. 41 No. 4**, 219-226. Equivalence Criteria between Mechanical Environments.

[2] B. FOX, L.S. JENNINGS AND A.Y. ZOMAYA 1999 IEEE *Transactions on Biomedical Engineering* **Vol. 46 No. 10**, 1199-1206. Numerical Computation of Differential-Algebraic Equations for Nonlinear Dynamics of Multibody Android Systems in Automobile Crash Simulation.

[3] M. GÉRADIN AND D. RIXEN 1994 *Mechanical Vibrations, Theory and Application to Structural Dynamics.* Paris, France : Masson.

[4] C. LALANNE 1999 *Vibrations et chocs mécaniques, Vibrations sinusoïdales (Tome 1).* Paris, France : HERMES Science Publications.

[5] C. LALANNE 1999 *Vibrations et chocs mécaniques, Chocs mécaniques (Tome 2).* Paris, France : HERMES Science Publications.

[6] C. LALANNE 1999 *Vibrations et chocs mécaniques, Vibrations aléatoires (Tome 3).* Paris, France : HERMES Science Publications.

[7] A. LINDER, M. AVERY, M. KRAFFT AND A. KULLGREN 2003 *Proceedings of the Eighteenth International Technical Conference on the Enhanced Safety of Vehicles, Nagoya, Japan.* Change of Velocity and Pulse Characteristics in Real Impacts : Real World and Vehicle Tests Data.

[8] LMS INTERNATIONAL 2009 *LMS Test.Lab Rev 9B Environment Testing Manual.* Leuven, Belgium.

[9] SAMTECH S.A. 2007 *SAMCEF 12.1 User's Guide.* Liège, Belgium.